

Promotion of in Vitro Hair Cell-like Cell Differentiation from Human Embryonic Stem Cells through the Regulation of Notch Signaling

Fengjiao Chen (✉ 997328451@qq.com)

Guizhou University <https://orcid.org/0000-0002-0995-4607>

Ying Yang

Guizhou University

Jianling Chen

Lishui University

Zihua Tang

Thermo Fisher Scientific

Qian Peng

University of Chinese Academy of Science

Jinfu Wang

Zhejiang University

Jie Ding

Guizhou University <https://orcid.org/0000-0002-0443-5111>

Research Article

Keywords: Human embryonic stem cells, progenitor cells, hair cell-like cells, Notch signaling pathway, shRNA

Posted Date: October 1st, 2021

DOI: <https://doi.org/10.21203/rs.3.rs-935209/v1>

License:   This work is licensed under a Creative Commons Attribution 4.0 International License.

[Read Full License](#)

Version of Record: A version of this preprint was published at Metabolites on December 15th, 2021. See the published version at <https://doi.org/10.3390/metabo11120873>.

Abstract

Background Notch signaling mediates the committed induced differentiation of ear sensory cells and promotes the formation of a precise arrangement of mosaics between hair cells and supporting cells. Embryonic stem cells (ESCs) are pluripotent stem cells which have the potential to differentiate into cell lines through three germ layers. Therefore, it is necessary to study the effects of regulating Notch receptors and ligand expression on the in vitro differentiation equilibrium of hair cells and supporting cells from ESCs.

Methods and Results The temporal expression pattern of Notch ligands and receptors during in vitro hair cell-like cell differentiation from human embryonic stem cells (hESCs) was detected by quantitative reverse transcription-polymerase chain reaction (qRT-PCR). Subsequently, pAJ-U6-shRNA-CMV-Puro/GFP recombinant lentiviral vectors, encoding short hairpin RNAs, were used to silence JAG-1, JAG-2, and DLL-1, according to the temporal expression pattern of Notch ligands. Then the effect of each ligand on the in vitro differentiation of hair cells was examined by RT-PCR, immunofluorescence, and scanning electron microscopy (SEM).

Conclusions Results showed that JAG-1 played an important role in regulating hESC differentiation to otic progenitors. The individual deletion of JAG-2 or DLL-1 had no significant effect on the differentiation of hair cell-like cells. Although the simultaneous inhibition of both DLL-1 and JAG-2 could increase the number of hair cell-like cells, it decreased the number of supporting cells.

1 Introduction

The Notch signaling pathway plays an important role in determining cell fate and function, including proliferation, differentiation and apoptosis, physiological and pathological processes, such as embryonic development, immunoregulation, tissue remodeling and tumorigenesis [1–3]. Activation of the Notch signaling pathway resulted in the lateral inhibition of cellular differentiation through interactions between the extracellular domain of the Notch proteins and membrane-bound ligands (such as Delta, Serrate, and Jagged) on neighboring cells [4]. Thus, this inhibitory interaction with the neighboring cells creates a mosaic cell pattern from initially homogenous cells. In addition, it has been verified that Notch signaling plays a number of roles in the development and regeneration of the inner ear in vertebrates [5–7]. Notch signaling mediates that the committed induced differentiation of ear sensory cells such as inner ear hair cells and supporting cells from equivalent otic progenitor cells (OPCs), and promoted the formation of a precise arrangement of mosaics between hair cells and supporting cells [8, 9]. NOTCH1 is an expression receptor at different stages of inner ear development, and Notch ligands involved in the differentiation of hair cells and supporting cells include Delta-like1 (DLL-1), Jagged1 (JAG-1), and Jagged2 (JAG-2) [10, 11]. Differential spatio-temporal expression pattern of Notch receptors and ligands during inner ear development indicates that the activation of Notch signaling pathway during different stages of development and through distinct Notch ligands might have a diverse role in hair cell and supporting cell differentiation [10, 12, 13]. Activation of the Notch signaling pathway during the early development of the

inner ear is propitious for the differentiation of otic progenitors. In the later development of the auditory epithelium, however, Notch signaling mediates alternate differentiation fates of equivalent OPCs through lateral inhibition. Specifically, OPCs with activated Notch signaling tend to differentiate into supporting cells, whereas OPCs with inhibited Notch signaling tend to differentiate into hair cells.

Embryonic stem cells (ESCs) are pluripotent stem cells which could differentiate into different cell lines through the ectoderm, mesoderm and endoderm [14]. With respect to hair cell regeneration, it was reported that the differentiation of human embryonic stem cells (hESCs) induced *in vitro* produced hair cell-like cells and auditory neurons [15]. Under the induction of fibroblast growth factor (FGF), hESCs were differentiated into inner ear progenitor cells and express a variety of hair cell markers [16]. In addition, hESCs were induced to differentiate into hair cell-like cells with statically cilia bundles [17]. As such, it is important to study the expression pattern of Notch receptors and ligands during *in vitro* differentiation of hair cells from ESCs, and the effects of regulating Notch ligand expression on the *in vitro* differentiation equilibrium of hair cells and supporting cells. Here, we examined the temporal expression pattern of Notch ligands and receptors during hair cell differentiation from hESCs. According to this temporal expression pattern, we constructed recombinant lentiviral shRNA vectors targeting JAG-1, JAG-2, and DLL-1. These lentivectors expressing JAG-1-, JAG-2-, and DLL-1-specific short hairpin RNAs (shRNAs) were transfected into the hESCs during different phases of *in vitro* hair cell-like cell differentiation. Subsequently, the effects of shRNA-mediated gene silencing (of Notch ligands) on the *in vitro* differentiation of hair cell-like cells were analyzed by RT-PCR, immunocytochemistry, and SEM. This finding could offer a theoretical foundation for research on the regulation of the *in vitro* differentiation equilibrium between hair cells and supporting cells derived from hESCs.

2 Materials And Methods

2.1 Two-step induction to generate hair cell-like cells from hESCs

The hESC line X1, obtained from Prof. Xiao, College of Animal Science, Zhejiang University, was cultured on inactivated mouse embryonic fibroblast (MEF) feeder cells with DMEM/F12 supplemented with 20% knockout serum replacement (KOSR; Gibco, Shanghai, China), 1% nonessential amino acids, 2 mM L-glutamine (Invitrogen, Shanghai, China), 0.1 mM 2-mercaptoethanol (Sigma, Shanghai, China), 50 mg/ml ampicillin, and 4 ng/ml of basic fibroblast growth factor (bFGF; Invitrogen). Before induction of the differentiation, the hESCs were dissociated into small clumps using collagenase IV (Invitrogen), and these small clumps were further dissociated using 0.025% trypsin-EDTA (Sigma). The tryptic digestion was terminated using a trypsin inhibitor, and the cell suspension was passed through a 100- μ m cell strainer (BD Labware, Shanghai, China) to retain few clumps of two to three cells.

For otic progenitor differentiation, cells were plated at the density of 1×10^4 cells/cm² on laminin-coated plastic (5 μ g/cm²; R&D systems, Shanghai, China) and incubated in DMEM/F12 supplemented with N2

(1:100), B27 (1:50), FGF3 (50 ng/ml), and FGF10 (50 ng/ml (Invitrogen) for 12 days. The medium was replaced with fresh medium every two days. After 12 days of differentiation, most hESCs had differentiated into otic progenitor cells. There were two morphologically distinct types of otic colonies [18]. One cell population exhibited a flat phenotype with a large amount of cytoplasm and formed epithelioid islands; these were identified as otic epithelial progenitors (OEPs). The second population had small cells with denser chromatin, and presented cytoplasmic projections; this population was identified as otic neural progenitors (ONPs). To enrich OEPs, cells surrounding the epithelial colony were lifted by a quick incubation with Accutase (Invitrogen), at 37°C for 2–3 min. As colony edges started to curl, cells surrounding the epithelial colonies were rinsed off. A prolonged accutase treatment step permitted the collection of epithelial colonies that remained attached. For induction of OEPs to differentiate into hair cell-like cells, we used laminin (Invitrogen) as a substrate [17]. Briefly, conditioned medium was used for hair cell differentiation. The conditioned medium was from a chicken utricle stromal cell culture and was supplemented with EGF (20 ng/ml) and RA (10^{-6} M). The conditioned medium was replaced every second day.

2.2 The expression pattern of genes specific for Notch signaling was analyzed during the different stages of hESC differentiation to hair cell-like cells.

Total RNA was extracted using Trizol reagent (TaKaRa, Shanghai, China) from cells in different stages of otic progenitor differentiation (otic progenitor differentiation for 6 and 12 days) and hair cell differentiation (hair cell differentiation for 5, 10, 12, 14, 16, 18, and 20 days). After reverse transcribing, the expression at mRNA level of Notch signaling pathway receptor NOTCH1 and ligands JAG1, JAG2, DLL1 were analyzed by quantitative real-time polymerase chain reaction (qRT-PCR), which was performed with LightCycler 480 using the default thermal cycling conditions (10 min at 95°C and 45 cycles of 15 s at 95°C plus 1 min at 60°C). HPRT1 and B2M were used as the endogenous control genes used for normalization. Relative quantification was performed using the comparative Ct (threshold cycle) method.

2.3 Recombinant lentiviral vector construction and cell transfection

To target different regions of each mRNA sequence (Table S1), four shRNAs targeting four different sequences of JAG-1, JAG-2, and DLL-1 (JAG-1-shRNA 1–4 for JAG-1, JAG-2-shRNA 1–4 for JAG-2, and DLL-1-shRNA 1–4 for DLL-1) and one negative control vector (NC-shRNA) were constructed by Jikai Genetics (Shanghai, China) (Table S2). Each shRNA sequence was inserted into the lentiviral vector (pAJ-U6-CMV-Puro/GFP) to construct the recombinant lentiviral vector pAJ-U6-shRNA-CMV-Puro/GFP. Subsequently, three plasmids pAJ-U6-shRNA-CMV-Puro/GFP, psPAX2 (gag/pol element), and pMD2.G (VSVG element) were transfected into 293T cells using Lipofectamine 3000 to generate Lenti-shRNA-GFP/puro viral particles. Reliable real-time PCR protocols were performed to titrate the lentivirus based on the number of proviral DNA copies present in the genomic DNA extracted from transduced cells or from

vector RNA. These production and concentration methods resulted in high-titer vector preparations (Table 1). Subsequently, JAG-1-recombinant lentiviral vectors were used to infect cells on day 12 of otic progenitor differentiation. JAG-2-recombinant lentiviral vectors or DLL-1-recombinant lentiviral vectors were used to infect cells on day 5 of hair cell differentiation. After 48 h, total RNA was extracted from these cells to perform qRT-PCR to analyze gene silencing efficiency. Then, the shRNA with the highest knockout efficiency was selected, we selected lentiviral vectors harboring these shRNAs to infect cells on day 6 and 12 of otic progenitor differentiation, and on day 5 of hair cell differentiation. After 48 h of infection, the cells were collected, filtered through a 300-mesh cell strainer, and suspended in 500 μ L DMEM/F12 (minus phenol red) supplemented with 10 μ M Y-27632, 200 U/ml penicillin, and 200 μ g/ml streptomycin. GFP-expressing cells were then sorted by flow cytometry (FCM). To unify the timing of sorting, we started the differentiation procedure at different times to ensure the time consistency of infection, collection, and sorting for all conditions. The sorted cells infected on day 6 of otic progenitor differentiation were cultured under the required conditions for an additional 6 days. Subsequently, some cells were collected for the analysis of otic progenitor differentiation, and other cells were transferred to laminin-coated plastic containing conditioned medium supplemented with EGF (20 ng /ml), RA (10^{-6} M), and Y-27632 (10 μ M) for 20 days of hair cell differentiation. The sorted cells infected on day 12 of otic progenitor differentiation and on day 5 of hair cell differentiation were directly transferred to laminin-coated plastic containing the conditioned medium supplemented with EGF (20 ng /ml), RA (10^{-6} M), and Y-27632 (10 μ M) for 15 and 20 days of hair cell differentiation. The medium was replaced with fresh medium every second day. Cells infected with lentivirus containing NC-shRNA were used as a control for analysis on the effects of each gene silence on the differentiation by qRT-PCR.

Table 1
Analysis of lentivirus titers by quantitative PCR

Lentivirus	Item	V Value	C Value	N Value	D Value	Viral titer	Mean titer
JAG-1-shRNA2	1	10	37	1×10^5	1	3.70E + 08	
	2	1	3.98	1×10^5	1	3.98E + 08	3.70E + 08
	3	0.1	0.34	1×10^5	1	3.40E + 08	
JAG-2-shRNA4	1	10	32	1×10^5	1	3.20E + 08	
	2	1	3.52	1×10^5	1	3.52E + 08	3.20E + 08
	3	0.1	0.29	1×10^5	1	2.90E + 08	
DLL-1-shRNA3	1	10	27.6	1×10^5	1	2.76E + 08	
	2	1	3.05	1×10^5	1	3.05E + 08	2.74E + 08
	3	0.1	0.24	1×10^5	1	2.40E + 08	
NC-shRNA	1	10	42	1×10^5	1	4.20E + 08	
	2	1	4.46	1×10^5	1	4.46E + 08	4.19E + 08
	3	0.1	0.39	1×10^5	1	3.90E + 08	

2.4 Western blot

Cells were washed twice with ice-cold PBS and protein was extracted. The extract was centrifuged at 12,000 rpm for 15 min at 4°C to remove cellular debris. Protein concentrations were determined by the Bradford method where in 20 µg of protein sample was heated to 95°C for 5 min, run on 10% SDS-PAGE gel, and transferred to PVDF membrane (Millipore, Shanghai, China) using the semidry transfer method. The membranes were blocked for 1 h in Tris-buffered saline containing 0.01% Tween 20 with 10% non-fat dried milk and incubated overnight at 4°C with the relevant antibodies including anti-DLL-1, anti-JAG-1, and anti-JAG-2 (Santa Cruz Biotechnology, Shanghai, China). After washing, the membranes were incubated with a peroxidase-conjugated anti-IgG secondary antibody, (Bio-Rad Laboratories, Shanghai, China) for 1 h. Protein bands were detected using an enhanced chemiluminescence detection kit. All the bands were analyzed using Image J software (version 1.6 NIH) to determine the relative levels of Notch signaling ligands compared to β-actin expression.

2.5 Gene expression specific analysis

Total RNA was extracted and reverse transcribed (Fermentas, Shanghai, China). The cDNA was used as a template for PCR using the primer pairs listed in Table 2. All RT-PCR results presented were confirmed by

at least two independent controlled experiments. PCR products were electrophoresed on a 1.2% agarose gel, and stained bands were visualized under UV light and photographed. Band intensities were analyzed quantitatively in triplicate using Image J software, and the expression level of each gene was normalized to that of GAPDH.

Table 2
Primers of RT-PCR for marker genes specific for otic progenitors and hair cells

Gene	Primer	Sequence	Tm
Sox2	Sense	5'- GGG AAA TGG GAG GGG TGC AAA AGA GG -3'	57°C
	Antisense	5'- TTG CGT GAG TGT GGA TGG GAT TGG TG -3'	
Oct4	Sense	5'- GAC AGG GGG AGG GGA GGA GCT AGG - 3'	58°C
	Antisense	5'- CCT CCC TCC AAC CAG TTG CCC CAA AC -3'	
Nanog	Sense	5'- ACC TAT GCC TGT GAT TTG - 3'	60°C
	Antisense	5'- AGA AGT GGG TTG TTT GC -3'	
Pax8	Sense	5'- ACC CCC AAG GTG GTG GAG AAG A -3'	62°C
	Antisense	5'- CTC GAG GTG GTG CTG GCT GAA G -3'	
Pax2	Sense	5'- GAG CGA GTT CTC CGG CAA C -3'	60°C
	Antisense	5'- GTC AGA CGG GGA CGA TGT G -3'	
Six1	Sense	5'- GAC TCC GGT TTT CGC CTT TG -3'	57°C
	Antisense	5'- TAG TTT GAG CTC CTG GCG TG -3'	
GATA3	Sense	5'-GTA CAG CTC CGG ACT CTT CCC-3'	60°C
	Antisense	5'- CTG CTC TCC TGG CTG CAG ACA - 3'	
Dlx5	Sense	5'- TTC CAA GCT CCG TTC CAG AC -3'	57°C
	Antisense	5'- GTA ATG CGG CCA GCT GAA AG -3'	
Eya-1	Sense	5'- TCA GAT GCT ATC TGC CGC TG -3'	57°C
	Antisense	5'- GTG CCA TTG GGA GTC ATG GA -3'	
Atoh1	Sense	5'- GCC GCC CAG TAT TTG CTA CA -3'	57°C
	Antisense	5'- GCT AGC CGT CTC TGC TTC TG -3'	
Myosin7A	Sense	5'- CAC ATC TTT GCC ATT GCT GAC - 3'	55°C
	Antisense	5'- AGA AGA GAA CCT CAC AGG CAT - 3'	
Espn	Sense	5' - CAG GCA TGT CCT CAC CCA AT -3'	55°C
	Antisense	5'- CGT GGC GGA GTT TGT TCT TG -3'	
Brn3c	Sense	5'- TGC AAG AAC CCA AAT TCT CC -3'	55°C
	Antisense	5'- GAG CTC TGG CTT GCT GTT CT -3'	
P27 ^{kip1}	Sense	5'- CTG GAG CGG ATG GAC GCC AGA C -3'	62°C

Gene	Primer	Sequence	Tm
	Antisense	5'- CGT CTG CTC CAC AGT GCC AGC - 3'	
GAPDH	Sense	5'- GAA GGT CGG AGT CAA CGG - 3'	58°C
	Antisense	5'- GGA AGA TGG TGA TGG GAT T-3'	

2.6 Immunocytochemistry

Cells were fixed with 4% paraformaldehyde for 15 min and permeabilized with PBS containing 0.25% Triton X-100 and 5% normal donkey serum for 10 min at room temperature. Blocking was performed in PBS containing 1% bovine serum albumin and 0.1% Tween-20, which was followed by three washes of 5 min each with PBS. The cells were incubated with primary antibody overnight at 4°C. After washing, specific antibody binding was visualized with donkey anti-mouse, anti-goat, or anti-rabbit secondary antibodies conjugated to either Alexa Fluor 488 or Alexa Fluor 594 (Jackson, Shanghai, China). The dilution ratio of all antibodies was based on the reference [17]. Nuclei were visualized with DAPI (4',6-diamidino-2-phenylindole). Images were acquired with a Zeiss Axiophot fluorescence and confocal microscope.

2.7 SEM assay

Cells differentiated for 3 weeks were fixed overnight in 2.5% glutaraldehyde (Sigma) at 4°C. The specimens were washed twice with PBS for 20 min each and treated with 1% osmium tetroxide (Sigma) for 30 min. The specimens were washed with PBS for 10 min and dehydrated in a graded ethanol series. Thereafter, ethanol was replaced with isoamyl acetate (Aladdin, Shanghai, China) for 20–30 min, and the specimens were dried using critical point drying method. The specimens were viewed with a Hitachi S-3000N variable pressure SEM.

2.8 Statistical analysis

Data are presented as mean values \pm standard deviation (SD) with the number of independent experiments (n) indicated. All collected data were examined by multifactorial analysis of variance. Statistical differences between the independent variables were assessed by post hoc tests (Tukey's studentized range tests for variables). All tests were two-tailed, and statistical significance was set at $P < 0.05$.

3 Results

3.1 Temporal expression pattern of Notch ligands and receptors during hESC hair cell differentiation

Examining the temporal expression pattern of Notch ligands and receptors during hair cell differentiation from hESCs was necessary to study the effects of Notch ligand gene silencing on the *in vitro* differentiation of hair cell-like cells. qRT-PCR was used to analyze the expression pattern of Notch ligands (*JAG-1*, *JAG-2*, and *DLL-1*) and receptor (*NOTCH1*) at the indicated times during the differentiation of hair cell-like cells from hESCs (Fig. 1). The results indicated that the expression of *JAG-1* mRNA was upregulated during the mid-stage of otic progenitor differentiation (from hESCs to otic progenitors) and downregulated during the mid-stage of hair cell differentiation (from otic progenitors to hair cell-like cells). The expression of *JAG-2* was upregulated during the early stage of hair cell differentiation and downregulated during the mid-stage of hair cell differentiation. Expression of *DLL-1* was initiated at the early stage of hair cell differentiation and ended at the mid-later stage. *Notch-1* mRNA was consistently detected throughout the differentiation of hESCs into hair cell-like cells and was finally downregulated during the final stage of hair cell differentiation. This expression pattern of Notch ligands and receptors during differentiation from hESCs to hair cell-like cells offered an important theoretical foundation for examining the effects of shRNA-mediated gene silencing of Notch ligands on the *in vitro* differentiation of hair cell-like cells.

3.2 The effects of shRNA silencing on the expression of target genes

Three series of lentiviral shRNA vectors (*JAG-1*-shRNA 1–4, *JAG-2*-shRNA 1–4, and *DLL-1*-shRNA 1–4) targeting four different sequences each of *JAG-1*, *JAG-2*, and *DLL-1* genes, and one negative control vector (NC-shRNA) were constructed. To determine the shRNA species with the highest silencing efficiency for each series of vectors, *JAG-1*-shRNA 1–4 vectors were used to infect cells on day 12 of otic progenitor differentiation, whereas *JAG-2*-shRNA 1–4 and *DLL-1*-shRNA 1–4 vectors were separately used to infect cells on day 5 of hair cell differentiation. Total RNA was then extracted from these cells 48 h after transfection to perform qRT-PCR. Results showed that *JAG-1*, *JAG-2*, and *DLL-1* in control (no transfection) and NC-shRNA transfected cells were expressed at the same levels ($P > 0.05$). The expression of *JAG-1*, *JAG-2*, and *DLL-1* in cells transfected with *JAG-1*-shRNA 1–4, *JAG-2*-shRNA 1–4 and *DLL-1*-shRNA 1–4 vectors was downregulated relative to that of the control ($P < 0.01$), respectively. *JAG-1*-shRNA2, *JAG-2*-shRNA4, and *DLL-1*-shRNA3 had the highest silencing efficiency of their corresponding genes (Fig. S1). Therefore, *JAG-1*-shRNA2, *JAG-2*-shRNA4, and *DLL-1*-shRNA3 vectors were chosen for subsequent stable infection.

After culturing in monolayers with otic progenitor-induction conditions for 10–12 days, hESCs can differentiate into two types of cells, OEPs and ONPs. OEPs were separated, and induced the hair cell differentiation for 3–4 weeks. To examine the effects of Notch signaling on the *in vitro* differentiation of hair cell-like cells, lentivirus (pAJ-U6-shRNA-CMV-Puro/GFP) -expressing *JAG-1*-shRNA2, *JAG-2*-shRNA4, or *DLL-1*-shRNA3 was used to infect cells at different stages of differentiation. Six infection schemes were performed according to the aforementioned Notch ligand expression patterns during differentiation of hESCs into hair cell-like cells, which included: J1-6d / J1-12d, designed such that cells on day 6 / 12 of

otic progenitor differentiation were infected with JAG-1-shRNA2; J2-5d / D1-5d / J2 + D1-5d, designed such that cells on day 5 of hair cell differentiation were infected with JAG-2-shRNA4 / DLL-1-shRNA3 / JAG-2-shRNA4 + DLL-1-shRNA3. After infection for 48h, the efficiency of GFP expression in each infection scheme was detected as shown in Fig. S2.

After stably infected cells from each scheme were sorted by FACS, the GFP-expressing of JAG-1, JAG-2, and DLL-1 were assessed by Western blotting. In addition to cells infected with NC-shRNA, uninfected cells were used as a control. The results showed that the JAG-1 expression in cells of both the J1-6d and J1-12d schemes was significantly lower than that in control schemes ($P < 0.05$). There was no significant difference in JAG-1 expression levels between the two control schemes ($P > 0.05$; Fig. S3 A and S3 B). In addition, JAG-2 and DLL-1 expressions in cells of the J2-5d and D1-5d schemes were significantly lower than that of both control schemes ($P < 0.05$; Fig. S3 C and S3 D). Moreover, both JAG-2 and DLL-1 expression in cells of the J2 + D1-5d scheme was significantly lower than that of both control schemes ($P < 0.05$; Fig. S3 E). These results confirmed the downregulation of JAG-1, JAG-2, and DLL-1 in the differentiating cells infected with corresponding shRNAs.

3.3 The expression of early otic-specific genes in otic progenitors infected with JAG-1-shRNA2

To study the function of JAG-1 in the *in vitro* differentiation of otic progenitors derived from hESCs, cells on day 6 of otic progenitor differentiation were infected with JAG-1-shRNA2 and cultured for another 6 days under otic progenitor-inducing condition. As shown in Fig. 2A and 2B, the specific expression levels of *Pax2*, *Pax8*, *Eya1*, *Six1*, and *Dlx5* in cells from the J1-6d infection scheme were significantly lower than those in cells infected with NC-shRNA by Semi-quantitative RT-PCR ($P < 0.01$). Therefore, the interference with JAG-1 could inhibit hESC differentiation into otic progenitors.

The effect of JAG-1 on the differentiation of otic progenitors was further defined by immunostaining with antibodies specific for Pax2 and Pax8 in cells from the J1-6d infection scheme (Fig. 2C₁ and 2C₂). The results demonstrated that the percentage of Pax8/Pax2 double-positive cells in the J1-6d infection scheme ($46.5 \pm 2.4\%$) was significantly lower than that of cells infected with NC-shRNA ($81.2 \pm 3.5\%$), which was in accordance with the RT-PCR analysis. This further validated that the downregulation of JAG-1 could inhibit hESC differentiation into otic progenitors.

3.4 Analysis of hair cell-specific markers and morphological characteristics

To examine the effects of silencing various Notch ligands on hair cell differentiation from hESCs, total RNA was extracted from cells, which were induced to undergo hair cell differentiation for 20 days, and was used to perform semi-quantitative RT-PCR. The expression of hair cell-specific genes (*Myosin7a*, *Brn3c*, *Atoh1*, and *Espin*) and one gene specific to supporting cells (*P27^{Kip1}*) were analyzed as shown in Fig. 3A and B. In cells of the J1-6d infection scheme, the expression levels of hair cell- or supporting cell-specific genes were all significantly lower than those in the cells infected with NC-shRNA ($P < 0.01$). There

was no significant difference in gene expression between cells from the J1-12d infection scheme and cells infected with NC-shRNA ($P > 0.05$) (Fig. 3B). Therefore, JAG-1 downregulation during otic progenitor differentiation not only inhibited hESC differentiation into otic progenitors, but also inhibited the differentiation and development of hair cells. However, interference with JAG-1 after the completion of otic progenitor differentiation had no significant effect on the differentiation of hair cell-like cells. The results demonstrated that JAG-1 primarily regulates the proliferation and differentiation of otic progenitors. In cells of the J2-5d and D1-5d infection schemes, the expression levels of hair cell- and supporting cell-specific genes were not significantly different from those of the cells infected with NC-shRNA ($P > 0.05$) (Fig. 3B). However, in cells induced from the J2 + D1-5d infection scheme, the expression of genes specific for hair cells was significantly higher than that of the cells infected with NC-shRNA, and the expression of $p27^{kip1}$ was significantly lower than that of the cells infected with NC-shRNA ($P < 0.05$) (Fig. 3B). These results showed that the downregulation of only one ligand (JAG-2 or DLL-1) could not significantly enhance the *in vitro* differentiation of hair cell-like cells, whereas interference with both ligands significantly upregulated the expression of hair cell-specific genes, which demonstrated that JAG-2 and DLL-1 together play a role in the regulation of *in vitro* hair cell differentiation.

Subsequently, immunofluorescence staining was performed on cells induced for 20 days to undergo hair cell differentiation, using antibodies specific for Atoh1, Brn3c, and Espin (targeting proteins specific for hair cells) to analyze the effects of Notch ligands on *in vitro* hair cell differentiation. The results showed that all cells expressing Brn3c were immunolabeled by Atoh1. The percentage of Brn3c/Atoh1 double-positive cells in the total cell population from the J1-6d infection scheme ($23.4 \pm 4.1\%$) was significantly lower than that of the cells infected with NC-shRNA ($82.6 \pm 3.4\%$). There was no significant difference in the percentage of Brn3c-Atoh1 double-positive cells between any of the four infection schemes (J1-12d, $79.2 \pm 3.7\%$; J2-5d, $84.1 \pm 2.6\%$; D1-5d, $85.3 \pm 2.1\%$; J2 + D1-5d, $87.2 \pm 4.3\%$) and the control scheme (Fig. 3C₁ and 3C₂). In addition, the fluorescence intensities of Brn3c and Atoh1 in the Brn3c/Atoh1 double-positive cells from the J2 + D1-5d infection scheme were much higher than those of Brn3c/Atoh1 double-positive cells from the other four infection schemes. This was consistent with differences in Brn3c and Atoh1 expression among the five infection schemes, as shown in Fig. 3B. Cells from the five infection schemes were also simultaneously labeled with antibodies specific for Brn3c and Myosin7a. As shown in Fig. 3D₁ and 3D₂, Myosin7a-positive cells were not detected in the J1-6d infection scheme. The percentage of cells co-expressing Brn3c and Myosin7a in the total cell population from the J1-12d infection scheme ($49.2 \pm 4.3\%$) and the fluorescence intensity in some Myosin7a-positive cells were slightly lower than those of the cells infected with NC-shRNA ($62.7 \pm 3.8\%$). In addition, the fluorescence intensity of Myosin7a in some Myosin7a-positive cells from the J2 + D1-5d infection scheme ($81.5 \pm 3.9\%$) was significantly higher than that of the cells infected with NC-shRNA. There was no significant difference in the positivity or fluorescence intensity between the other two infection schemes (J2-5d, $65.1 \pm 2.7\%$ and D1-5d, $67.3 \pm 4.0\%$) and the control scheme. Then cells from the five infection schemes were analyzed for the co-expression of Brn3c and Espin as shown in Fig. 3E₁ and 3E₂. Espin-positive cells were not detected in the J1-6d infection scheme. Cells from the control, J1-12d, J2-5d, D1-5d, and J2 + D1-5d

infection schemes contained $5.8 \pm 2.3\%$, $4.7 \pm 2.9\%$, $6.4 \pm 1.8\%$, $6.1 \pm 2.6\%$, and $9.3 \pm 2.4\%$ Espin-positive cells, respectively. In all the cells of the five infection schemes, Espin was mainly distributed in bundles at one side of the cell resembling stereociliary bundles. The percentage of Brn3C/Espin double positive cells from the two infection schemes (J2-5d, $6.4 \pm 1.8\%$ and D1-5d, $6.1 \pm 2.6\%$) was not significantly different from that of the cells infected with NC-shRNA (Fig. 3E₁ and 3E₂). Only the percentage of Espin-positive cells in the J2 + D1-5d infection scheme was higher than that of the cells infected with NC-shRNA ($P < 0.05$).

Finally, SEM was selected to examine the structure and morphology of stereocilia on the surface of hair cell-like cells from the six infection schemes. As shown in Fig. 4, cells from the J1-12d, J2-5d, D1-5d, and J2 + D1-5d infection schemes had stereocilia-like structures and some stereocilia were bundled together with their tip-links (Fig. 4E–L). This result was similar to that observed in control cells (Fig. 4A and 4B). However, stereocilia were not detected on the surface of cells from the J1-6d infection scheme (Fig. 4C and 4D). Therefore, JAG-1 blocked not only suppressed otic progenitor differentiation, but also inhibited stereocilia-like structure formation on the surface of the induced cells.

4 Discussion

ShRNA, transduced by lentivirus, can be expressed stably in infected cell lines [19–21]. Therefore, lentivirus-harboring shRNA was packaged, concentrated, and infected into the targeted cells to produce efficient and long-term gene silencing [22–24]. In this study, the constructed lentiviral shRNA vector was transfected into target cells. The vector with the highest interference efficiency to the three genes (JAG-1, JAG-2 and DLL-1) was selected by real-time PCR: JAG-1-shRNA2, JAG-2-shRNA4 and DLL-1-shRNA3 [25, 26]. Subsequently, the proportion of GFP positive cells sorted by FACS showed that the infection efficiency on day 6 and 12 of otic progenitor differentiation was higher than that on day 5 of hair cell differentiation. This implies that otic progenitors should be easily infected by lentivirus. However, Western blotting to assess knockdown efficiency showed that the expression levels of targeted proteins in all infection schemes were significantly lower than that in the no transfection and NC-shRNA schemes, as expected.

The activation of Notch signaling pathway promotes the formation of otic precursor cells during the early development of the inner ear. However, Notch signaling leads to two different cell fates in adjacent otic precursors through lateral inhibition during the subsequent development of the auditory sensory epithelium [7, 27]. Otic precursors activated by Notch signaling differentiate into supporting cells, whereas those inhibited by Notch signaling differentiate into hair cells. Moreover, Co-activation of cell cycle activator and Notch effectively transdifferentiated into mature supporting cells into hair cells [28, 29]. The prominent function of JAG-1 in Notch signaling is lateral induction, which is essential for the proliferation and development of otic progenitors and is necessary for hair cell differentiation [30–35]. Macchiarulo et al. found that knocking out JAG-1 in mouse ear canal vesicles led to failure of semicircular tube development and reduction of hair cells [36]. In the inner ear of the mouse, DLL-1 and JAG-2 inhibit differentiation into hair cells in adjacent otic progenitors and promote these cells to differentiate into

supporting cells [37, 38]. The simultaneous deletion of JAG-2 and DLL-1 leads to the loss of supporting cells as well as promotes the development and large number of hair cells [39, 40], which was consistent with the lateral inhibition hypothesis. While the quantity of hair cells was not obviously changed when either JAG-2 or DLL-1 were individually deleted [6, 10, 41]. It has been speculated that JAG-2 and DLL-1 might play a synergistic role in the development of hair cells [10]. However, studies on the function of Notch signaling during the *in vitro* development, differentiation of hair cells and supporting cells from pluripotent stem cells are rare. Therefore, the expression pattern of Notch signaling during the *in vivo* differentiation of hair cells and supporting cells, as well as the effects of regulating Notch signaling on the *in vivo* differentiation of the two kinds of cells require further investigation. In this study, JAG-1 was expressed in the mid-stage of otic progenitor differentiation. Therefore, downregulation of JAG-1 was induced in cells at day 6 and 12 of otic progenitor differentiation (designated as J1-6d and J1-12d infection schemes, respectively). Subsequently, cells on day 12 of otic progenitor differentiation and day 20 of hair cell and supporting cell differentiation were analyzed by detecting the expression of genes specific to otic progenitors or differentiated cells, to study the effect of JAG-1 on *in vitro* hair cell and supporting cell differentiation. For cells at day 12 of otic progenitor differentiation, the expression of otic progenitor-specific genes and proteins in the J1-6d infection scheme was significantly lower than that of the control cells. The GFP-positive cells in the J1-6d and J1-12d infection schemes were sorted by FACS and were eventually induced to differentiate into hair cell-like cells. Cells at day 20 of hair cell differentiation were analyzed by RT-PCR, immunocytochemistry, and SEM. The results showed that the expression of hair cell-specific genes and proteins in cells from the J1-6d infection scheme was significantly lower than that of the control cells, and no stereocilia-like structures were detected on the surface of these cells. Similarly, the expression of supporting cells-specific genes was significantly downregulated. However, not only the expression of hair cell-specific genes and proteins in the cells of the J1-12d infection protocol was slightly lower than that of the control, but also the gene expression of supporting cells, while their differences were not significant. In addition, stereocilia-like structures could be detected. These results demonstrated that during the process of *in vitro* hair cell differentiation (from hESCs), downregulation of JAG-1 at the otic progenitor differentiation stage blocks the differentiation of otic progenitors, thus indirectly reducing the number of hair cell-like cells and supporting cells. Inhibition of JAG-1 expression in mature otic progenitors had no significant effect on the differentiation of hair cells and supporting cells. Therefore, we speculated that JAG-1 involved in the differentiation of otic progenitors and promotes the differentiation and development of these cells.

During *in vitro* differentiation, JAG-2 and DLL-1 were detected in hair cells on day 5 of the differentiation. Therefore, JAG-2 and DLL-2 were downregulated individually (J2-5d and D1-5d infection schemes) or simultaneously (J2 + D1-5d infection scheme) in cells on day 5 of hair cell differentiation. Cells on day 20 of hair cell differentiation were analyzed by detecting the expression of genes or proteins and assessing stereociliary structure formation, which is specific for hair cells to examine the role of JAG-2 and DLL-1 in the *in vitro* differentiation of hair cell-like cells. Downregulation of JAG-2 or DLL-1 in cells in the early stage of hair cell and supporting cell differentiation had no significant effect on the differentiation potential. In addition, stereocilia on the surface of cells derived from J2-5d, D1-5d, and J2 + D1-5d

infection schemes were well distributed and we observed the existence of stereocilia-like structures with links between the tips of these structures, on the surface of hair cell-like cells. This was similarly observed in cells of the control scheme. The expression of hair cell-specific genes and proteins was significantly higher when JAG-2 and DLL-1 were simultaneously downregulated, while the expression of supporting cell-specific genes was downregulated. These results suggest that JAG-2 and DLL-1 play an important role in the *in vitro* differentiation of otic progenitors into hair cells and supporting cells, and perhaps inhibit the differentiation and development of hair cells. Downregulation of only one of these ligands (JAG-2 or DLL-1) did not significantly increase the *in vitro* differentiation of hair cell-like cells; however, interference with both the ligands could significantly increase the differentiation of hair cells and promote the formation of stereocilia bundle-like structures on the surface of induced hair cells. This demonstrated that JAG-2 and DLL-1 might have a synergistic role in the regulation of hair cell-like cell differentiation. As such, gene interaction may promote the regeneration of hair cells, and the mechanism of regulating the differentiation of Notch signaling pathway in hair cells and supporting cells is worthy of further study. Undoubtedly, targeted gene therapy to help the hearing function recovery of people with sensorineural deafness will also become an attractive option for future research.

5 Conclusion

The two-step induction protocol for generating hair cell-like cells from hESCs was used in this study. The first induction step is for the differentiation of hESCs into otic progenitors, whereas the second induction step is for the differentiation of OEPs into hair cell-like cells. Lentiviruses expressing JAG-1-, JAG-2- and DLL-1-shRNA were used to infect cells in different phases of hair cell differentiation to silence specific Notch ligand genes. During the differentiation of otic progenitors, the downregulation of JAG-1 expression hindered otic progenitor differentiation and further resulted in insufficient differentiation into hair cell-like cells. The downregulation of JAG-1 expression in mature otic progenitors had no significant impact on hair cell and supporting cell differentiation. During the differentiation of hair cell-like cells, the downregulation of JAG-2 and DLL-1 could not significantly increase the differentiation potentials of the cells. However, hair cell differentiation was significantly promoted and supporting cell differentiation was restricted when JAG-2 and DLL-1 were simultaneously downregulated. These results demonstrate that JAG-2 and DLL-1 might have a synergistic role in *in vitro* hair cell differentiation.

Abbreviations

hESCs, human embryonic stem cells; OEPs, otic epithelial progenitors; ONPs, otic neural progenitors; shRNAs, short hairpin RNAs; RNAi, RNA interference; SEM, scanning electron microscopy; MEF, mouse embryonic fibroblast; KOSR, knockout serum replacement; FGF3, Fibroblast growth factor 3; FGF10, Fibroblast growth factor 10; bFGF, basic fibroblast growth factor; EGF, epidermal growth factor; RA: all-trans retinoic acid; RT-PCR, reverse transcription-polymerase chain reaction; FCM, flow cytometry; GFP, green fluorescent protein.

Declarations

Author contributions

F.J.C., Y.Y., J.D., J.L.C., Z.H.T., Q.P. : performed the experiments and contributed to the data analysis. J.D. and J.F.W drafted the study, designed the experiments, and monitored the project progression, the data analysis and the data interpretation. J.D.: prepared the initial draft of the manuscript. J.F.W.: prepared the final version of the manuscript.

Funding

Partial financial support was received from National Basic Research Program of China (2014CB541705), Basic Research Program of Guizhou science and Technology ([2021]108), Basic Research Program of Guizhou science and Technology ([2017]7266), Talent growth project of Guizhou Education Department (KY[2017]113), Talent introduction Program of Guizhou University[2016(35)], The Guizhou Province Graduate Research Fund (YJSCXJH[2020]080).

Data availability

All data generated or analysed during this study are included in this published article (and its supplementary information files).

Conflict of interest

None.

Compliance with Ethical Standards

The authors declare that they have no conflict of interest. All procedures performed in studies involving human participants were in accordance with the ethical standards of the institutional and/or national research committee and with the 1964 Helsinki declaration and its later amendments or comparable ethical standards. This article does not contain any studies with animals performed by any of the authors. Informed consent was obtained from all individual participants included in the study.

Consent to participate

All participants signed an informed consent form.

Consent to publication

All participants signed informed consent.

References

1. Yu J, Canalis E (2020) Notch and the regulation of osteoclast differentiation and function. *Bone* 138:115474. <https://doi.org/10.1016/j.bone.2020.115474>
2. McCarter AC, Wang Q, Chiang M (2018) Notch in Leukemia. *Adv Exp Med Biol* 1066: 355–394. https://doi.org/10.1007/978-3-319-89512-3_18
3. Meurette O, Patrick M (2018) Notch Signaling in the Tumor Microenvironment. *Cancer Cell* 34 (4): 536–548. <https://doi.org/10.1016/j.ccell.2018.07.009>
4. Bray SJ (2006) Notch signalling: a simple pathway becomes complex. *Nat Rev Mol Cell Bio* 7(9):678–689. <https://doi.org/10.1038/nrm2009>
5. Tateya T, Sakamoto S, Imayoshi I, Kageyama R (2015) In vivo overactivation of the Notch signaling pathway in the developing cochlear epithelium. *Hearing. Res* 327:209–217. <https://doi.org/10.1016/j.heares.2015.07.012>
6. Brown R, Groves AK (2020) Hear, Hear for Notch: Control of Cell Fates in the Inner Ear by Notch Signaling. *Biomolecules* 10(3):370. <https://doi.org/10.3390/biom10030370>
7. Daudet N, Žak M (2020) Notch Signalling: The Multitask Manager of Inner Ear Development and Regeneration. *Adv Exp Med Biol* 1218:129–157. https://doi.org/10.1007/978-3-030-34436-8_8
8. Munnamalai V, Fekete DM (2016) Notch-Wnt-Bmp crosstalk regulates radial patterning in the mouse cochlea in a spatiotemporal manner. *Development* 143(21): 4003–4015. <https://doi.org/10.1242/dev.139469>
9. Hanae L, Alejandra L, Arnaud F, Emmanuel N, Azel Z (2018) Modeling human early otic sensory cell development with induced pluripotent stem cells. *Plos One* 13(6):e0198954. <https://doi.org/10.1371/journal.pone.0198954>
10. Murata J, Ikeda K, Okano H (2012) Notch signaling and the developing inner ear. *Adv Exp Med Biol* 727:161–173. https://doi.org/10.1007/978-1-4614-0899-4_12
11. Jiang H, Zeng S, Ni W, Chen Y, Li WY (2019) Unidirectional and stage-dependent roles of Notch1 in Wnt-responsive Lgr5 + cells during mouse inner ear development. *Front Med-prc* 13(6):705–712. <https://doi.org/10.1007/s11684-019-0703-y>
12. Lin V, Golub JS, Nguyen TB, Hume CR, Oesterle EC, Stone JS (2011) Inhibition of Notch activity promotes nonmitotic regeneration of hair cells in the adult mouse utricles. *J Neurosci* 31:15329–15339. <https://doi.org/10.1523/JNEUROSCI.2057-11>
13. Petrovic J, Gálvez H, Neves J, Abelló G, Giraldez F (2015) Differential regulation of Hes/Hey genes during inner ear development. *Dev Neurobiol* 75(7): 703–720. <https://doi.org/10.1002/dneu.22243>

14. Ko E, Hwang KA, Choi KC (2019) Prenatal toxicity of the environmental pollutants on neuronal and cardiac development derived from embryonic stem cells. *Reprod Toxicol* 90: 15–23. <https://doi.org/10.1016/j.reprotox.2019.08.006>
15. Chen W, Jongkamonwiwat N, Abbas L, Eshtan SJ, Johnson SL, Kuhn S, Milo M, Thurlow JK, Andrews PW, Marcotti W, Moore HD, Rivolta MN (2012) Restoration of auditory evoked responses by human ES-cell-derived otic progenitors. *Nature* 490(7419):278–282. <https://doi.org/10.1038/nature11415>
16. Ronaghi M, Nasr M, Ealy M, Durruthy DR, Waldhaus J, Diaz GH, Joubert LM, Oshima K, Heller S (2014) Inner ear hair cell-like cells from human embryonic stem cells. *Stem Cells Dev* 23(11): 1275–1284. <https://doi.org/10.1089/scd.2014.0033>
17. Ding J, Tang ZH, Chen JR, Shi HS, Chen JL, Wang CC, Zhang C, Li L, Chen P, Wang JF (2016) Induction of differentiation of human embryonic stem cells into functional hair-cell-like cells in the absence of stromal cells. *Int J Biochem Cell Biol* 81:208–222. <https://doi.org/10.1016/j.biocel.2015.11.012>
18. Daudet N, Ariza-McNaughton L, Lewis J (2007) Notch signalling is needed to maintain, but not to initiate, the formation of prosensory patches in the chick inner ear. *Development* 134:2369–2378. <https://doi.org/10.1242/dev.001842>
19. Jiang L, Zhang JH, Hu NF, Liu AC, Zhu HL, Li LQ, Tian YY, Chen X, Quan LN (2018) Lentivirus-mediated down-regulation of CK2 α inhibits proliferation and induces apoptosis of malignant lymphoma and leukemia cells. *Biochem Cell Biol* 96(6):786–796. <https://doi.org/10.1139/bcb-2017-0345>
20. Levin AA (2019) Treating Disease at the RNA Level with Oligonucleotides. *New Engl J Med* 380(1):57–70. <https://doi.org/10.1056/NEJMra1705346>
21. Bao YL, Feng HJ, Zhao FP, Zhang LJ, Xu SG, Zhang CH, Zhao C, Qin G (2021) FANCD2 knockdown with shRNA interference enhances the ionizing radiation sensitivity of nasopharyngeal carcinoma CNE-2 cells. *Neoplasma* 68(1):40–52. https://doi.org/10.4149/neo_2020_200511N516
22. Zhao HM, He L, Yin DX, Song B (2019) Identification of β -catenin target genes in colorectal cancer by interrogating gene fitness screening data. *Oncol Lett* 18(4):3769–3777. <https://doi.org/10.3892/ol.2019.10724>
23. Forster H, Shuai B (2020) Exogenous siRNAs against chitin synthase gene suppress the growth of the pathogenic fungus *Macrophomina phaseolina*. *Mycologia* 112(4):699–710. <https://doi.org/10.1080/00275514.2020.1753467>
24. He WT, Tu M, Du YH, Li JJ, Pang YY, Dong ZF (2020) Nicotine Promotes A β PP Nonamyloidogenic Processing via RACK1-Dependent Activation of PKC in SH-SY5Y-A β PP695 Cells. *J Alzheimers Dis* 75(2):451–460. <https://doi.org/10.3233/JAD-200003>
25. Ma T, Pei YZ, Li CG, Zhu MX (2019) Periodicity and dosage optimization of an RNAi model in eukaryotes cells. *Bmc bioinformatics* 20(1):340. <https://doi.org/10.1186/s12859-019-2925-z>
26. Ma J, Chen SJ, Qin Y, Zhang YY, Sun XF (2021) In vivo and in vitro Experiment of E74-Like Factor 5 Overexpression Inhibiting the Biological Behavior of Colon Cancer Cells. *Journal of Sichuan*

- University (Medical science edition) 52(3):430–437. <https://doi.org/10.12182/20210560207>
27. Juan CLE, Pau FJ, Marta I (2018) Redundancy and cooperation in Notch intercellular signaling. *Development* 145(1):dev154807. <https://doi.org/10.1139/bcb-2017-0345>
 28. Shu YL, Li WY, Huang MQ, Quan YZ, Scheffer D, Tian CJ, Tao Y, Liu SZ, Hochedlinger K, Indzhukulian AA, Wang ZM, Li HW, Chen ZY (2019) Renewed proliferation in adult mouse cochlea and regeneration of hair cells. *Nat Commun* 10(1):5530. <https://doi.org/10.1038/s41467-019-13157-7>
 29. Seiji BS, Matthew BWest, Xiaoping D, Yoichiro I, Yehoash R, Richard DK (2020) Gene therapy for hair cell regeneration: Review and new data. *Hearing Res* 394:107981. <https://doi.org/10.1016/j.heares.2020.107981>
 30. Byron HH, Thomas AR, Olivia BM, Gail M (2010) Notch signaling specifies prosensory domains via lateral induction in the developing mammalian inner ear. *P Natl Acad Sci Usa* 107(36):15792–15797. <https://doi.org/10.1073/pnas.1002827107>
 31. Hao J, Koesters R, Bouchard M, Gridley T, Pfannenstiel S, Plinkert PK, Zhang L, Praetorius M (2012) Jagged1-mediated Notch signaling regulates mammalian inner ear development independent of lateral inhibition. *Acta Oto-laryngol* 132(10):1028–1035. <https://doi.org/10.1371/10.3109/00016489.2012.690533>
 32. Neves J, Abello G, Petrovic J, Giraldez F (2013) Patterning and cell fate in the inner ear: a case for Notch in the chicken embryo. *Develop Growth Differ* 55(1): 96–112. <https://doi.org/10.1111/dgd.12016>
 33. Petrovic J, Formosa-Jordan P, Luna-Escalante JC, Abelló G, Ibañes M, Neves J, Giraldez F (2014) Ligand-dependent Notch signaling strength orchestrates lateral induction and lateral inhibition in the developing inner ear. *Development* 141(11):2313–2324. <https://doi.org/10.1242/dev.108100>
 34. Li Y, Jia SP, Liu HZ, Tateya T, Guo WW, Yang SM, Beisel KW, He DZZ (2018) Characterization of Hair Cell-Like Cells Converted From Supporting Cells After Notch Inhibition in Cultures of the Organ of Corti From Neonatal Gerbils. *Front Cell Neurosci* 12:73. <https://doi.org/10.3389/fncel.2018.00073>
 35. Brown RMII, Nelson JC, Zhang HY, Kiernan AE, Groves AK (2020) Notch-mediated lateral induction is necessary to maintain vestibular prosensory identity during inner ear development. *Dev Biol* 462(1):74–84. <https://doi.org/10.1016/j.ydbio.2020.02.015>
 36. Macchiarulo S, Morrow BE (2017) Tbx1 and Jag1 act in concert to modulate the fate of neurosensory cells of the mouse otic vesicle. *Biol Open* 6(10):1472–1482. <https://doi.org/10.1242/bio.027359>
 37. Kiernan AE, Cordes R, Kopan R, Gossler A, Gridley T (2005) The Notch ligands DLL-1 and JAG-2 act synergistically to regulate hair cell development in the mammalian inner ear. *Development* 132:4353–4362. <https://doi.org/10.1242/dev.02002>
 38. Redeker C, Schuster GK, Kremmer E, Gossler A (2018) Normal development in mice over-expressing the intracellular domain of DLL-1 argues against reverse signaling by DLL-1 in vivo. *Plos One* 8(10): e79050. <https://doi.org/10.1371/journal.pone.0079050>

39. Brooker R, Hozumi K, Lewis J (2006) Notch ligands with contrasting functions: Jagged1 and Delta1 in the mouse inner ear. *Development* 133(7):1277–1286. <https://doi.org/10.1242/dev.02284>
40. Slowik AD, Bermingham-McDonogh O (2013) Notch signaling in mammalian hair cell regeneration. *Trends Dev Biol* 7:73–89
41. Basch ML, Brown RM, Jen HI, Semerci F, Depreux F, Edlund RK, Zhang HY, Norton CR, Gridley T, Cole SE, Doetlhofer A, Maletic-Savatic M, Segil N, Groves AK (2016) Fine-tuning of Notch signaling sets the boundary of the organ of Corti and establishes sensory cell fates. *Elife* 5:e19921. <https://doi.org/10.7554/eLife.19921>

Figures

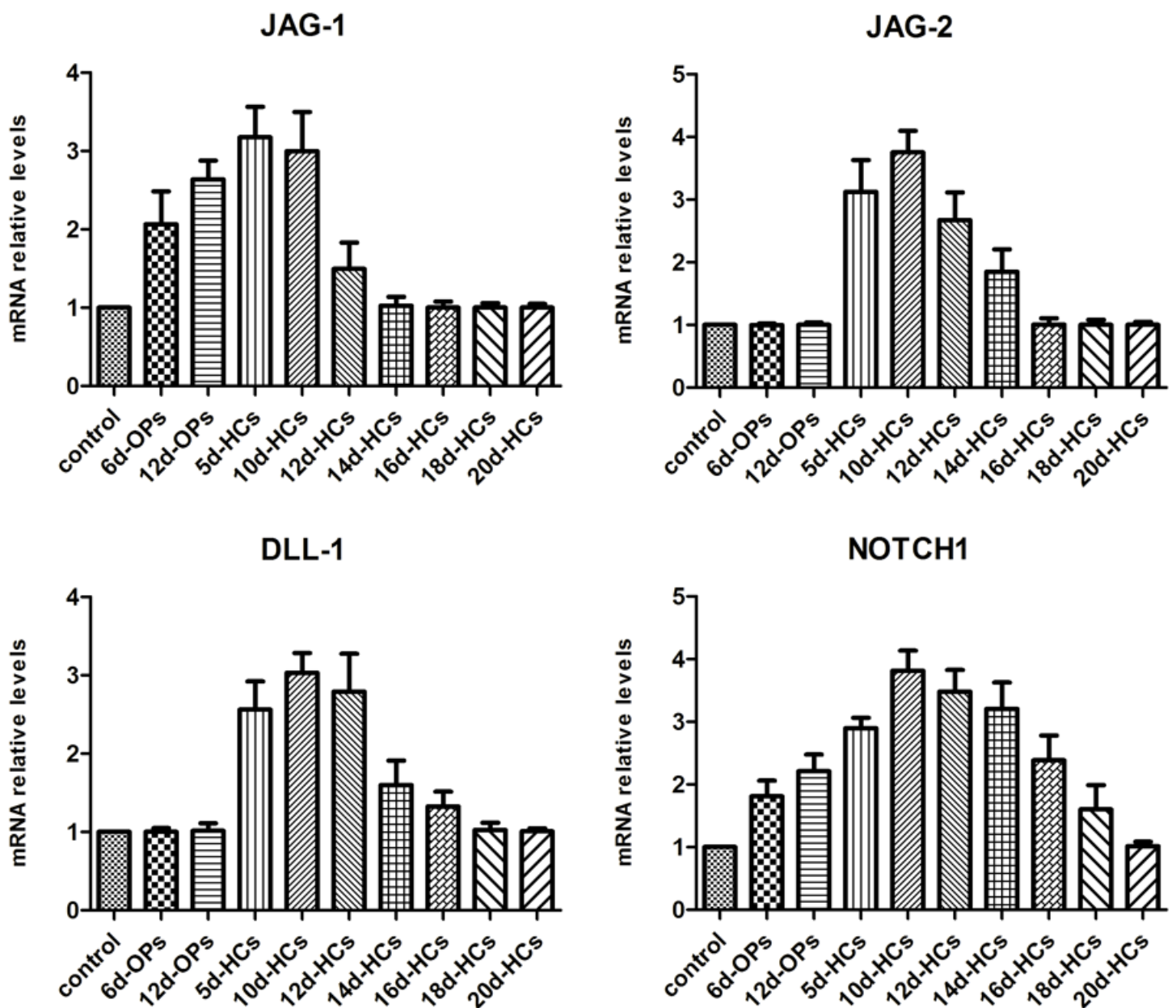


Figure 1

The expression pattern of Notch ligands and receptors. qRT-PCR analysis was performed to determine the expression pattern of Notch ligands and receptors. The expression of JAG-1 and NOTCH1 mRNA was gradually upregulated throughout the otic progenitor differentiation, whereas JAG-1 was downregulated during the mid-stage (day 14) and NOTCH1 was downregulated in the final stage (day 20) of hair cell differentiation. JAG-2 and DLL-1 mRNAs were detected at the early stage of hair cell differentiation, but their expression was downregulated by the mid-later stage of the differentiation. The statistical results were significant ($P < 0.05$). Control: Undifferentiated human embryonic stem cells; 6d-Ops / 12d-OPs: cells on day 6 / 12 of otic progenitor differentiation; 5d-HCs / 10d-HCs / 12d-HCs / 14d-HCs / 16d-HCs / 18d-HCs / 20d-HCs : cells on day 5 / 10 / 12 / 14 / 16 / 18 / 20 of hair cell differentiation.

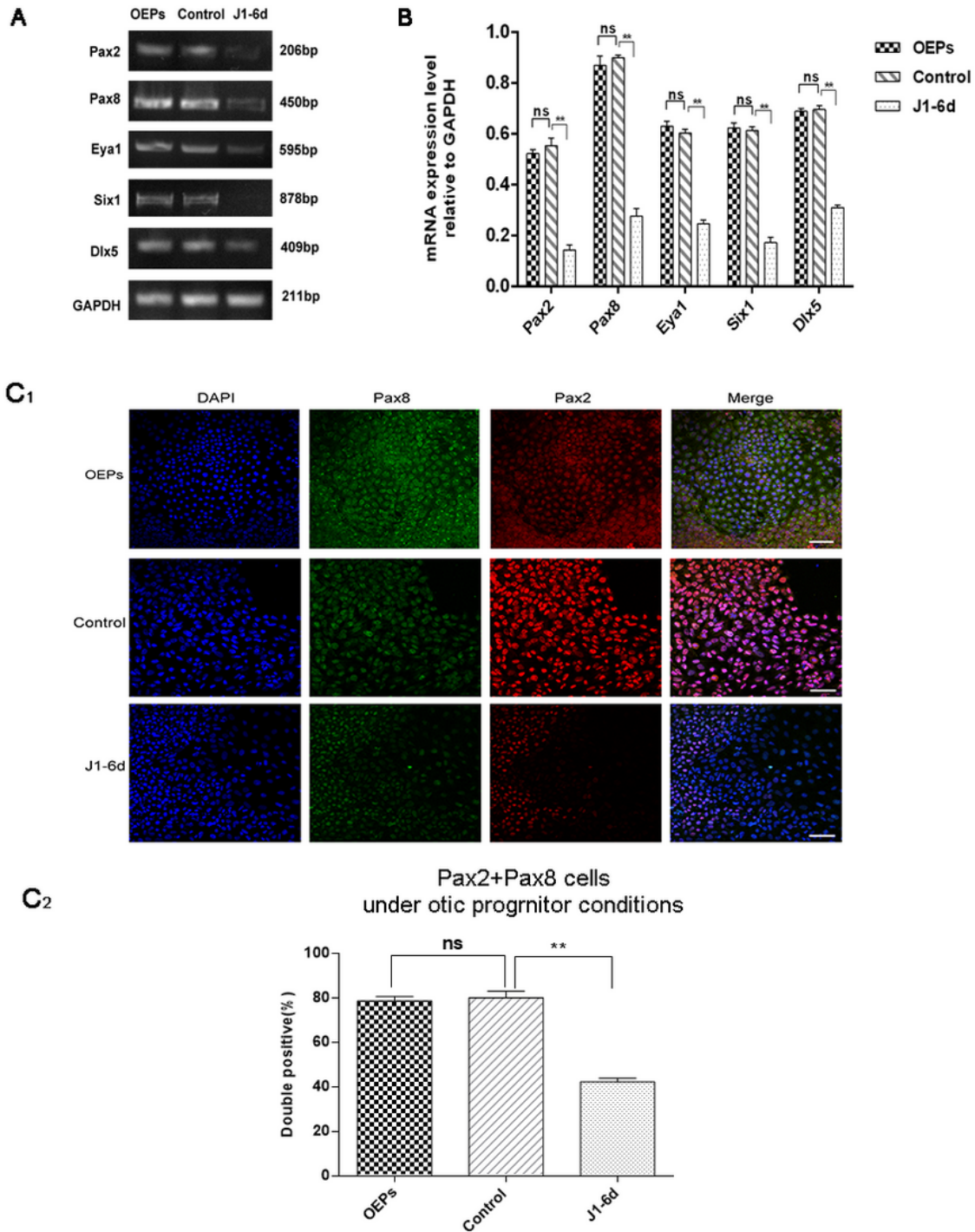


Figure 2

Analyses of early otic-specific markers in otic progenitors from the J1-6d infection scheme. (A) RT-PCR analyses for the expression of the early otic markers Pax2, Pax8, Dlx5, Six1, and Eya1. OEPs: no transfection. Control: cells infected by lentivirus with NC-shRNA on day 6 of otic progenitor differentiation. J1-6d: cells infected with lentivirus harboring JAG-1-shRNA2 at day 6 of otic progenitor differentiation and then cultured for another 6 days under otic progenitor-inducing conditions. (B) Semi-

quantitative analysis of the expression of specified genes by Image J and GraphPad. Expression values are relative to those of GAPDH and are presented as the mean \pm SD ($n = 3$). * indicates $P < 0.05$; ** indicates $P < 0.01$; *** indicates $P < 0.001$. (C1) Immunostaining of cells from the J1-6d infection scheme with antibodies specific for early otic markers. (C2) Co-expression of Pax2 and Pax8, specific for otic progenitors, in cells induced from the J1-6d infection scheme and control scheme. Error bars represent the SD ($n = 5$). The percentage of Pax8/Pax2 double-positive cells in the total cell population from the J1-6d infection scheme was significantly lower than that of the control scheme. Scale bar: 20 μ m.

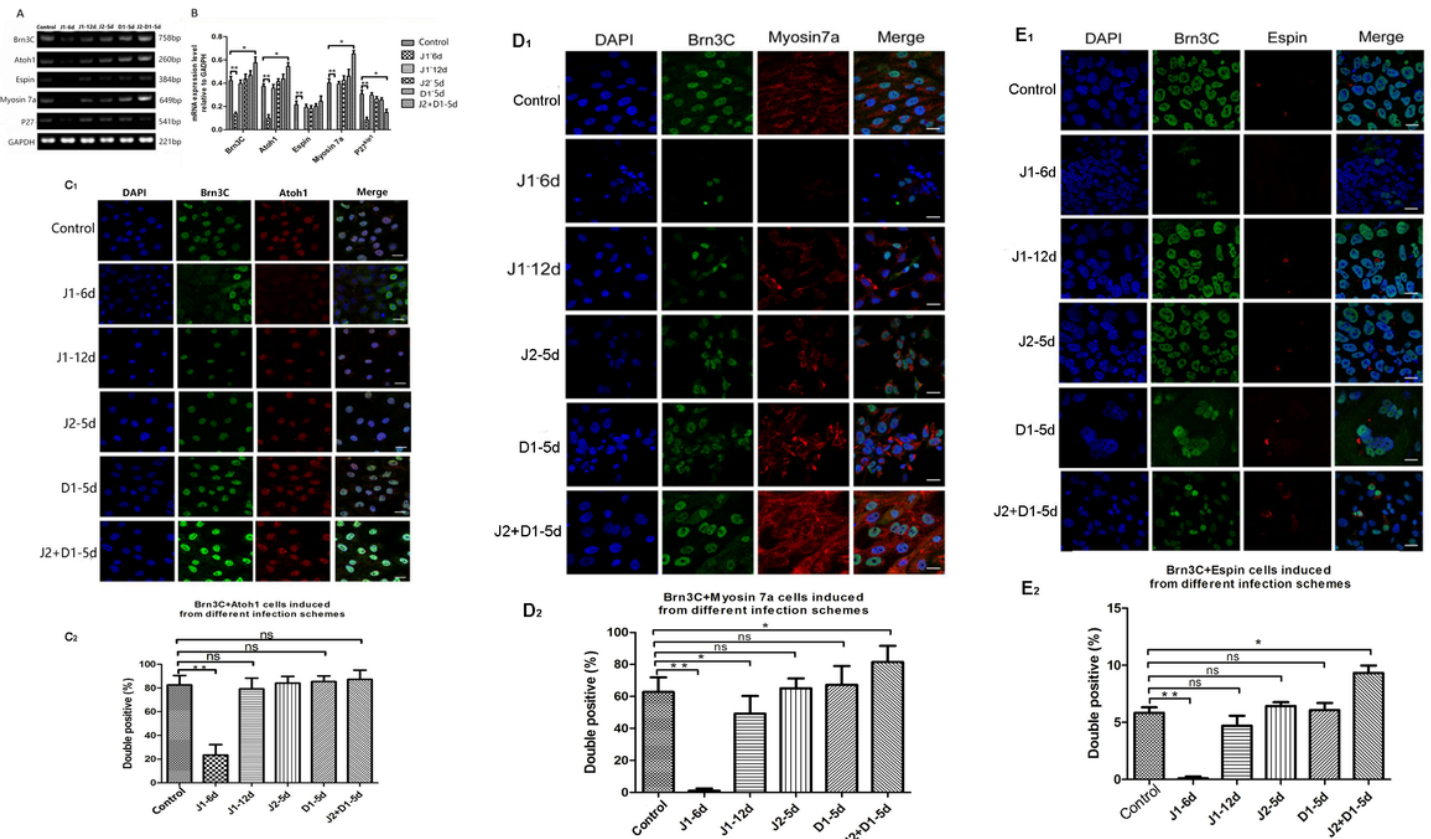


Figure 3

Analysis of hair cell- and supporting cell-specific markers in cells from six infection schemes. (A) RT-PCR analyses for the expression of markers specific for hair cells (Myosin7a, Brn3c, Atoh1, and Espin) and supporting cells (P27 kip1) in cells from six infection schemes. (B) Semi-quantitative analysis of the expression of specific genes using Image J and GraphPad. Expression values are relative to those of GAPDH and are presented as the mean \pm SD ($n = 3$). * indicates $P < 0.05$; ** indicates $P < 0.01$; *** indicates $P < 0.001$. (C1) Co-expression of Atoh1 (Red) and Brn3c (Green) in cells induced from six infection schemes. Scale bar: 20 μ m. (C2) Percentage of Brn3c/Atoh1 double-positive cells in total cells induced using different infection schemes. Error bars represent the SD ($n = 5$). (D1) Co-expression of Myosin7a (Red) and Brn3c (Green) in cells induced using the six infection schemes. Scale bar: 20 μ m. (D2) Co-expression of Brn3c and Myosin 7a in total cells induced using the different infection schemes. Error bars represent the SD ($n = 5$). (E1) Co-expression of Espin (Red) and Brn3c (Green) in cells induced

using the six infection schemes. Scale bar: 20 μm . (E2) Percentage of Brn3C/Espin double-positive cells in total cells induced using the different infection schemes. Error bars represent the SD (n = 5). Control: cells infected by lentivirus with NC-shRNA (cells infected by lentivirus with NC-shRNA on day 6 of otic progenitor differentiation are used as the representative of all controls. There is no significant difference of expression between different control conditions). J1-6d / J1-12d: cells infected with lentivirus harboring JAG-1-shRNA2 at day 6 / 12 of otic progenitor differentiation and harvested for analysis at day 20 of hair cell differentiation. J2-5d / D1-5d / J2+D1-5d : cells infected with lentivirus harboring JAG-2-shRNA4 / DLL-1-shRNA3 / JAG-2-shRNA4 + DLL-1-shRNA3 at day 5 of hair cell differentiation and harvested for analysis at day 20 of hair cell differentiation.

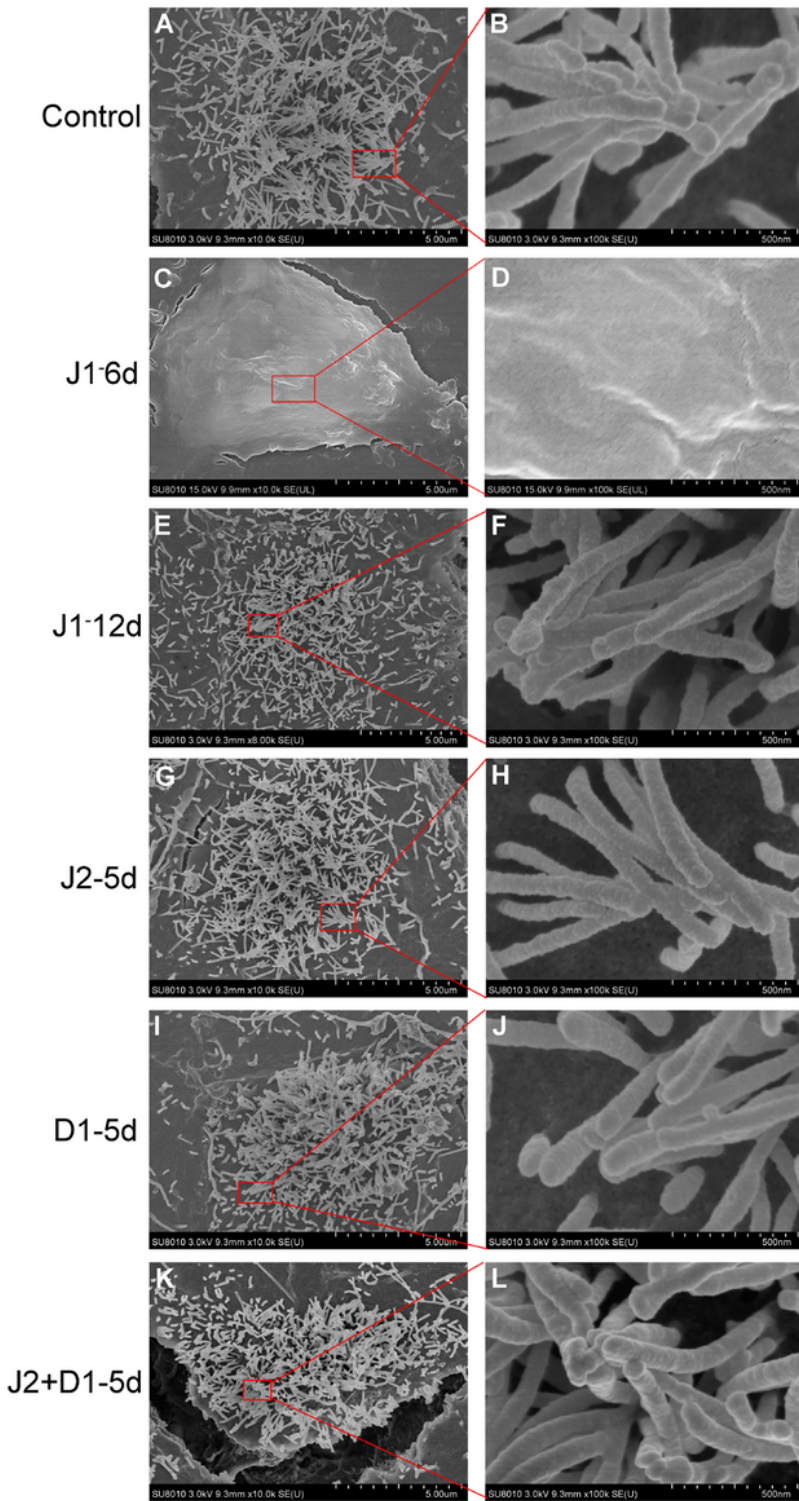


Figure 4

Scanning electron microscopy (SEM) analysis of hair cell-like cells from six infection schemes. (A-B) Stereocilia-like structures on the surface of hair cell-like cells induced from cells infected with NC-shRNA on day 6 of otic progenitor differentiation as the representative of all controls (Control). (C-D) No stereocilia-like structures were detected on the surface of hair cell-like cells induced using the J1-6d

infection scheme. Stereocilia-like structures on the surface of hair cell-like cells induced using the J1-12d (E-F), J2-5d (G-H), D1-5d (I-J), and J2+D1-5d (K-L) infection schemes.

Supplementary Files

This is a list of supplementary files associated with this preprint. Click to download.

- [SupplementalMaterial.docx](#)
- [SupplementalMaterial2.jpg](#)